Available online at http://scik.org
Commun. Math. Biol. Neurosci. 2026, 2026:70
https://doi.org/10.28919/cmbn/9943
ISSN: 2052-2541

ROLE OF WIND ON THE DYNAMIC OF STAGE STRUCTURED PREDATOR-PREY SYSTEM WITH CANNIBALISM

RASHA A. ALI[1,2], HIBA ABDULLAH IBRAHIM [1,*]

[1]Department of Mathematics, College of Science, University of Baghdad, Baghdad, Iraq

[2]Theoretical Sciences Department, College of Physical Education and Sports Science, University of Baghdad, Baghdad, Iraq

Abstract: This article presents a new mathematical model of a predator-prey ecosystem that contains biological relations such as wind flow, stage structure, and cannibalism. To perform the dynamic analysis of the system, the positivity and boundedness of the proposed system were examined, and feasible equilibrium points were found. By utilizing the linearization technique and Lyapunov functions, the local and global stability were established, respectively. All conditions for persistence were identified. By the bifurcation theory, the impacts of changing the parameters were examined. A numerical simulation was used to validate our analytical results by using MATLAB code (version R2018b). It is found that the impact of wind flow plays a major role in the dynamics of the system. When the wind flow increases, then the predators (mature and immature) become extinct, which means the effect of wind flow hinders the reduction and efficiency of predators. On the other hand, the cannibalism coefficient also affects the dynamics of the system, whereby the bistable state appears.

Keywords: cannibalism; persistence; stability analysis; stage structure; wind effect.

2020 AMS Subject Classification: 92D25, 34D20.

---

[*]Corresponding author
E-mail address: hiba.ibrahim@sc.uobaghdad.edu.iq
Received April 25, 2026

1. INTRODUCTION

After the publication of the famous mathematical model by [1,2], many research studies were conducted to explore the dynamics of predator-prey systems. Ecological systems are fundamentally shaped by predator-prey interactions that influence the structure of communities and the dynamics of populations.

Many factors affect the dynamics of the system, such as hunting cooperation [3,4], the fear effect [5-7], and disease [8,9]. To investigate the dynamics of ecosystems, the Holling Type II is widely utilized in these systems; see [10,11].

Therefore, to understand the dynamics of these systems, a considerable amount of research has focused on integrating predator-prey models with a Holling type II functional response; see [12-14]. Cannibalism is a biological phenomenon that can affect the existence of predator-prey relationships in ecosystems. Many studies have been published in this area [15-17]. In reality, several species have cannibalistic features, such as fish [18,19], spider [20,21] and carnivore mammals [22,23].

Cannibalism is a common trait of stage structured population. Many natural species have stage structured life cycles, typically with immature and mature phases. In stage structured predator-prey models, it's reasonable to assume that immature predators can't catch prey and depend on their parents.

The dynamic interactions between species with stage-structuring in ecological systems have garnered much interest in recent ecological and biological studies [24, 25]. When combined with elements like fear effects [26, 27], competition [28, 29], and infectious disease [30]. The intricate dynamics of predator-prey relationships create fascinating problems in comprehending ecosystem behaviors. Recently, a cannibalism model with stage structure has been discussed in [31]. Various bifurcations and stability analyses are taken into consideration. These studies emphasize the value of including complex ecological elements in mathematical models and the necessity of thorough stability and bifurcation analyses to clarify the fundamental mechanisms governing system dynamics. Researchers can gain crucial insights into the stability and behavior of predator-prey systems by carefully examining such complex dynamics, which will affect our understanding of ecological processes.

The dynamic of the predator-prey model with a modified Holling Type II response that includes the wind effect has been studied recently [32-35]. [32] proposed a predator-prey model with anti-predator behavior and wind flow. It was found that the influence of anti-predator behavior and wind flow can contribute to the stability of the system. Also, [33] suggested a food web model with prey and two competing predators under fear and wind flow. They found that the increase of fear led to a decrease of the predators, and the bi-stable case appeared, while increasing of wind flow led to the extinction of the predators.

A stage structured predator-prey system with cannibalism was presented. The effect of wind is incorporated into the Holling Type II functional response. Examining local stability, global stability, persistence, and bifurcation are all part of the model analysis process. It is essential to comprehend the dynamics of this system to forecast population trends and ecological results. This article is structured in these steps. The formulation of the mathematical model has been established in section 2. The positivity and boundedness are demonstrated in Section 3. A study on the existence of possible equilibria is examined in section 4. The stability analysis, both local and global, is discussed in sections 5 and 6, respectively. The persistence conditions are investigated in section 7. Bifurcation analysis of equilibria is done in section 8. Numerical analysis for parameters is in section 9. Finally, the conclusions of this work are illustrated in section 10.

2. MODEL FORMULATION

In this article, a stage structured predator-prey system under the wind flow and cannibalism is considered. Let $x(t)$ and $P(t)$ be the densities of the population prey and predator at time t, respectively. The predator population $P(t)$ is divided into immature $y(t)$ and mature $z(t)$. The population of prey grows logistically with the intrinsic growth rate; it is highly dependent on the carrying capacity. It is assumed that the immature predator can't reproduce or hunt, and its growth depends on its parents (the mature predator), while some grow to become mature (adult). The mature predator is feeding dependent on the prey, utilizing a modified Holling type II functional response under wind flow [36], and it cannibalizes on the immature predator utilizing Lotka-Volterra functional response when their favorite food becomes rare. Both the predators (mature and immature) face natural mortality. The dynamics of the predator-prey system can be described by using a set of ordinary differential equations (ODEs) as below:

$$\begin{aligned} \frac{dx}{dt} &= x\left[r\left(1-\frac{x}{k}\right)-\frac{\beta_1 z}{1+\omega+\alpha x}\right], \\ \frac{dy}{dt} &= \frac{e_1\beta_1 xz}{1+\omega+\alpha x}-\beta_2 yz-cy-d_1 y,, \\ \frac{dz}{dt} &= cy+e_2\beta_2 yz-d_2 z, \end{aligned} \tag{1}$$

where $x(t)\geq 0$, $y(t)\geq 0$, and $z(t)\geq 0$. The positive parameter descriptions are listed in Table

1).

Table 1. Description of Model Parameters

Symbols	Description
r	Intrinsic growth rate of the prey.
k	Carrying capacity of the prey.
β_1	The attack rate of a mature predator $z(t)$ on the prey $x(t)$.
ω	Wind flow
α	The hindrance rate in prey catching for the mature predator.
e_1	The conversion rate of $z(t)$ into $x(t)$.
β_2	The attack rate of the mature predator $z(t)$ on the immature predator $y(t)$.
c	The rate of growth from an immature predator into a mature predator.
d_1	The mortality rate of immature predator.
e_2	The conversion rate of $z(t)$ into $y(t)$.
d_2	The mortality rate of mature predator.

3. Positivity and Boundedness

The positivity and boundedness of system (1) solutions are essential properties of biological meaningfulness. The positivity of solutions indicates that the population will continue for a certain period, and since resources are limited, the population cannot grow beyond certain limits and is bound. This subsection discusses these properties.

Theorem 1. System (1) solutions $(x(t), y(t), z(t))$ starting from the initial conditions always remain non-negative in the domain R_+^3 for all $t \geq 0$.

Proof.

$$x(t) = x(0)exp\int_0^t \left[rx(\tau)\left(1-\frac{x(\tau)}{k}\right) - \frac{\beta_1 x(\tau)z(\tau)}{1+\omega+\alpha x(\tau)}\right]d\tau > 0,$$

$$y(t) = y(0)exp\int_0^t \left[\frac{e_1\beta_1 x(\tau)z(\tau)}{1+\omega+\alpha x(\tau)} - \beta_2 y(\tau)z(\tau) - cy(\tau) - d_1 y(\tau)\right]d\tau > 0\,,$$

$$z(t) = z(0)exp\int_0^t \left[cy(\tau) + e_2\beta_2 y(\tau)z(\tau) - d_2 z(\tau)\right]d\tau > 0.$$

This shows that system (1) solutions are always positive $\forall t \geq 0$.

Theorem 2. System (1) solutions $(x(t), y(t), z(t))$ starting from the initial conditions are uniformly bounded in the domain R_+^3 for all $t \geq 0$.

Proof. The first equation of system (1) can be written as

$$\frac{dx(t)}{dt} \leq rx\left(1-\frac{x}{k}\right) .$$

The previous differential inequality was solved, and it was obtained that

$$\lim_{t\to\infty} Sup\, x(t) \leq k.$$

Let $\Theta(t) = x(t) + y(t) + z(t)$ be a solution of system (1), by utilizing the derivative about t.

$$\frac{d\Theta}{dt} = \frac{dx}{dt} + \frac{dy}{dt} + \frac{dz}{dt}$$

$$= xr\left(1-\frac{x}{k}\right) - \frac{\beta_1 xz}{1+\omega+\alpha x} + \frac{e_1\beta_1 xz}{1+\omega+\alpha x} - \beta_2 yz - cy - d_1 y + cy + e_2\beta_2 yz - d_2 z,$$

$$\leq x(1+r) - x - d_1 y - d_2 z.$$

So, $\frac{d\Theta}{dt} \leq k(1+r) - \zeta\Theta$, where $\zeta = min\{1, d_1, d_2\}$ and this lead to $\frac{d\Theta}{dt} + \zeta\Theta \leq k(1+r)$.

Therefore, for $t \to \infty$, $\Theta(t) \leq \frac{k(1+r)}{\zeta}$.

Then the solutions of system (1) are uniformly bounded.

4. Equilibrium Points of System (1)

In this section, all biologically feasible equilibrium points of system (1) are investigated. It is clear that there are three equilibrium points of system (1), which can be determined as below:

1. The trivial equilibrium point (T-EP) referred to by $E_0 = (0,0,0)$ exists.
2. The Axial equilibrium point (A-EP) referred to by $E_1 = (k, 0,0)$ exists.
3. The coexistence equilibrium point (COE-EP) referred to by $E_2 = (x^*, y^*, z^*)$, here $y^* = \frac{rd_2(1-(x^*/k))(1+\omega+\alpha x^*)}{\beta_1 c + e_2\beta_2 r(1-(x^*/k))(1+\omega+\alpha x^*)}$, $z^* = \frac{r}{\beta_1}\left(1-(x^*/k)\right)(1+\omega+\alpha x^*)$, and x^* be a positive root of the polynomial's equation of order four

$$\sigma_1 x^4 + \sigma_2 x^3 + \sigma_3 x^2 + \sigma_4 x + \sigma_5 = 0, \tag{2}$$

where $\sigma_1 = \frac{r^2}{k^2}\beta_2\alpha(e_1e_2\beta_1 - d_2\alpha)$,

$$\sigma_2 = \frac{r^2}{k}\beta_2\left(e_1e_2\beta_1\left(\frac{1+\omega}{k} - 2\alpha\right) - 2\alpha d_2\left(\frac{1+\omega}{k} - \alpha\right)\right),$$

$$\sigma_3 = r\left[r\beta_2\left(e_1e_2\beta_1\left(\alpha - \frac{2(1+\omega)}{k}\right) - d_2\left(\alpha^2 - \frac{4(1+\omega)\alpha}{k} + \frac{(1+\omega)^2}{k^2}\right)\right) + \frac{\beta_1}{k}(d_2\alpha(c+d_1) - e_1\beta_1 c)\right],$$

$\sigma_4 = r\left[e_1\beta_1^2 c + r\beta_2(1+\omega)\left(e_1e_2\beta_1 - 2d_2\left(\alpha - \frac{1+\omega}{k}\right)\right) + \beta_1 d_2(c+d_1)\left(\frac{1+\omega}{k} - \alpha\right)\right]$,

$\sigma_5 = -d_2 r(1+\omega)\big(\beta_2 r(1+\omega) + \beta_1(c+d_1)\big)$.

By using Descartes' rule of signs, the COE-EP has a unique positive root if one set of the following sets of conditions holds:

$$\sigma_1 > 0, \sigma_3 < 0, \sigma_4 < 0, \tag{3}$$

$$\sigma_1 > 0, \sigma_2 > 0, \sigma_3 > 0, \tag{4}$$

$$\sigma_1 > 0, \sigma_2 > 0, \sigma_4 < 0. \tag{5}$$

Then, the COE-EP exists provided that the above conditions are met.

5. Local Stability Analysis

By using linearization technique, the local stability of all possible equilibrium points of system (1) is studied analytically, as shown in Theorem 3.

Theorem 3.

i. The T-EP is always unstable.
ii. The A-EP is locally asymptotically stable if condition (10) is met.
iii. The COE-EP is locally asymptotically stable if conditions (13-16) are met.

Proof: The Jacobian matrix of system (1) can be written as

$$\begin{pmatrix} r(1-\frac{x}{k}) - \frac{\beta_1 z}{1+\omega+\alpha x} + x(\frac{\alpha\beta_1 z}{(1+\omega+\alpha x)^2} - \frac{r}{k}) & 0 & -\frac{\beta_1 x}{1+\omega+\alpha x} \\ \frac{(1+\omega)e_1\beta_1 z}{(1+\omega+\alpha x)^2} & -(c+d_1+\beta_2 z) & \frac{e_1\beta_1 x}{1+\omega+\alpha x} - \beta_2 y \\ 0 & c + e_2\beta_2 z & e_2\beta_2 y - d_2 \end{pmatrix} \tag{6}$$

i. For the T-EP, the $J(E_0)$ can be written as

$$J(E_0) = \begin{pmatrix} r & 0 & 0 \\ 0 & -(c+d_1) & 0 \\ 0 & c & -d_2 \end{pmatrix} \tag{7}$$

The eigenvalues of $J(E_0)$ are $\lambda_{01} = r > 0$, $\lambda_{02} = -(c+d_1) < 0$, and $\lambda_{03} = -d_2 < 0$. Hence, $E_0 = (0,0,0)$ is an unstable (Saddle point).

ii. For the A-EP, the $J(E_1)$ can be written as

$$J(E_1) = \begin{pmatrix} -r & 0 & -\frac{k\beta_1}{1+\omega+\alpha k} \\ 0 & -(c+d_1) & \frac{ke_1\beta_1}{1+\omega+\alpha k} \\ 0 & c & -d_2 \end{pmatrix} \tag{8}$$

The characteristic equation is

$$(-r-\lambda)(\lambda^2 - Trace_1\lambda + Det_1) = 0, \tag{9}$$

Here, $Trace_1 = -(c + d_1 + d_2) < 0.$

$Det_1 = d_2(c + d_1) - \frac{cke_1\beta_1}{1+\omega+\alpha k}.$

Hence, the A-EP is locally asymptotically stable if the following condition is met.

$$\frac{cke_1\beta_1}{1+\omega+\alpha k} < (c + d_1)d_2 \tag{10}$$

iii. For the COE-EP, the $J(E_2)$ can be written as

$$J(E_2) = \begin{pmatrix} \epsilon_{11} & 0 & \epsilon_{13} \\ \epsilon_{21} & \epsilon_{22} & \epsilon_{23} \\ 0 & \epsilon_{32} & \epsilon_{33} \end{pmatrix}, \tag{11}$$

Where $\epsilon_{11} = x^*\left(-\frac{r}{k} + \frac{\alpha\beta_1 z^*}{(1+\omega+\alpha x^*)^2}\right)$, $\epsilon_{13} = -\frac{\beta_1 x^*}{1+\omega+\alpha x^*}$, $\epsilon_{21} = \frac{(1+\omega)e_1\beta_1 z^*}{(1+\omega+\alpha x^*)^2}$, $\epsilon_{22} = -(c + d_1 + \beta_2 z^*)$, $\epsilon_{23} = \frac{e_1\beta_1 x^*}{1+\omega+\alpha x^*} - \beta_2 y^*$, $\epsilon_{32} = c + e_2\beta_2 z^*$, and $\epsilon_{33} = e_2\beta_2 y^* - d_2$.

Then, the characteristic equation is

$$\lambda^3 + A_1\lambda^2 + A_2\lambda + A_3 = 0, \tag{12}$$

Where $A_1 = -(\epsilon_{11} + \epsilon_{22} + \epsilon_{33})$.

$A_2 = -(\epsilon_{23}\epsilon_{32} - \epsilon_{11}\epsilon_{22} - \epsilon_{11}\epsilon_{33} - \epsilon_{22}\epsilon_{33})$.

$A_3 = -(\epsilon_{11}\epsilon_{22}\epsilon_{33} + \epsilon_{13}\epsilon_{21}\epsilon_{32} - \epsilon_{11}\epsilon_{23}\epsilon_{32})$.

By apply the Routh-Hawirtiz Criterion [37], the roots of the characteristic equation (12) have negative real parts if the following conditions are met, $A_1 > 0$, $A_3 > 0$ and $\Delta = A_1A_2 - A_3 > 0$, where

$\Delta = -\epsilon_{11}\epsilon_{22}(\epsilon_{11} + \epsilon_{22}) - \epsilon_{11}\epsilon_{33}(\epsilon_{11} + \epsilon_{33}) - (\epsilon_{22} + \epsilon_{33})(\epsilon_{22}\epsilon_{33} - \epsilon_{23}\epsilon_{32}) + Q$.

Here, $Q = -2\epsilon_{11}\epsilon_{22}\epsilon_{33} + \epsilon_{13}\epsilon_{21}\epsilon_{32}$.

So, the COE-EP is locally asymptotically stable if the following conditions are met.

$$\frac{\alpha\beta_1 z^*}{(1+\omega+\alpha x^*)^2} < \frac{r}{k}, \tag{13}$$

$$\frac{e_1\beta_1 x^*}{1+\omega+\alpha x^*} < \beta_2 y^*, \tag{14}$$

$$e_2\beta_2 y^* < d_2, \tag{15}$$

$$Q > 0. \tag{16}$$

6. GLOBAL STABILITY ANALYSIS

In this section, the appropriate Lyapunov functions are used to describe the global stability of system (1), as shown in Theorem 4.

Theorem 4.

i. The A-EP is globally asymptotically stable if the following condition is met.

$$\frac{\beta_1 k}{1+\omega} < d_2. \tag{17}$$

ii. The COE-EP has a basin of attraction that satisfies the following conditions:

$$\frac{\beta_1(1+\omega)z^*}{qq^*} - r\left(1 - \frac{x+x^*}{k}\right) > 0, \tag{18}$$

$$e_2\beta_2 y < d_2, \tag{19}$$

$$p_{12}^2 < p_{11}p_{22}, \tag{20}$$

$$p_{13}^2 < p_{11}p_{33}, \tag{21}$$

$$p_{23}^2 < p_{22}p_{33}. \tag{22}$$

Proof:

i. Define an appropriate function

$$\Omega_1(x,y,z) = \int_k^x \frac{u-k}{u}\,du + y + z. \tag{23}$$

The function Ω_1 is a positive definite. So, $\Omega_1(k,0,0) = 0$ and $\Omega_1(x,y,z) > 0$, $\forall (x,y,z) \in \mathbb{R}_+^3\ with\ (x,y,z) \neq (k,0,0)$. Now, deriving (23) with respect to t, and through several calculations, it's got:

$$\frac{d\Omega_1}{dt} = (x-k)\left(r\left(1-\frac{x}{k}\right) - \frac{\beta_1 z}{1+\omega+\alpha x}\right) + \left(\frac{e_1\beta_1 xz}{1+\omega+\alpha x} - \beta_2 yz - cy - d_1 y\right) + (cy + e_2\beta_2 yz - d_2 z).$$

$$\frac{d\Omega_1}{dt} \leq \frac{-r}{k}(x-k)^2 - d_1 y - \left(d_2 - \frac{\beta_1 k}{1+\omega}\right) z.$$

Under condition (17), the derivative of $\Omega_1(x,y,z)$ will be negative definite. Therefore, Ω_1 is a Lyapunov function, and the A-EP is a globally asymptotically stable.

ii. Define an appropriate function

$$\Omega_2(x,y,z) = \frac{(x-x^*)^2}{2} + \frac{(y-y^*)^2}{2} + \frac{(z-z^*)^2}{2}. \tag{24}$$

The function Ω_2 is a positive definite. So, $\Omega_2(x^*,y^*,z^*) = 0$ and $\Omega_2(x,y,z) > 0$, $\forall (x,y,z) \in \mathbb{R}_+^3\ with\ (x,y,z) \neq (x^*,y^*,z^*)$. Now, deriving (24) with respect to t, and through several calculations, it's got:

$$\frac{d\Omega_2}{dt} = (x-x^*)\left(rx\left(1-\frac{x}{k}\right) - \frac{\beta_1 xz}{1+\omega+\alpha x}\right) + (y-y^*)\left(\frac{e_1\beta_1 xz}{1+\omega+\alpha x} - \beta_2 yz - cy - d_1 y\right)$$

$$+ (z-z^*)(cy + e_2\beta_2 yz - d_2 z)$$

$$\frac{d\Omega_2}{dt} = -p_{11}(x-x^*)^2 - p_{22}(y-y^*)^2 - p_{33}(z-z^*)^2 + p_{12}(x-x^*)(y-y^*) - p_{13}(x-x^*)(z-z^*) - p_{23}(y-y^*)(z-z^*)$$

Where $p_{11} = \frac{\beta_1(1+\omega)z^*}{qq^*} - r\left(1-\frac{x+x^*}{k}\right)$, $p_{22} = \beta_2 z^* + c + d_1$, $p_{33} = d_2 - e_2\beta_2 y$,

$p_{12} = \frac{e_1\beta_1(1+\omega)z^*}{qq^*}$, $p_{13} = \frac{\beta_1 x}{q}$, $p_{23} = \beta_2 y - \frac{e_1\beta_1 x}{q} - e_2\beta_2 z^* - c$.

With $q = 1+\omega+\alpha x$, $q^* = 1+\omega+\alpha x^*$.

Therefore,

$$\frac{d\Omega_2}{dt} \le -\left[\sqrt{\frac{p_{11}}{2}}(x-x^*) - \sqrt{\frac{p_{22}}{2}}(y-y^*)\right]^2 - \left[\sqrt{\frac{p_{11}}{2}}(x-x^*) + \sqrt{\frac{p_{33}}{2}}(z-z^*)\right]^2 - \left[\sqrt{\frac{p_{22}}{2}}(y-y^*) + \sqrt{\frac{p_{33}}{2}}(z-z^*)\right]^2.$$

As a result, $\frac{d\Omega_2}{dt}$ is a negatively definite function under conditions (18-22). Hence, all solutions approach asymptotically to the COE-EP within the region that satisfies the given conditions.

7. Persistence of System (1)

In this part, the persistence of system (1) is studied. Thus, system (1) is persistent when every species is present for all $t > 0$. In the following theorem, the Freedman and Waltman method that depends on the Butler-McGhie lemma is used of the system (1).

Theorem 5. System (1) is persistent if the following condition is met:

$$\frac{cke_1\beta_1}{1+\omega+\alpha k} > (c+d_1)d_2. \qquad (25)$$

Proof. Let m be a point $\in Int.R_+^3$ and $O(m)$ represent the orbit via m.

Let $\Omega(m)$ be the omega limit set of $O(m)$. Then, due to Theorem 1, $\Omega(m)$ is bounded.

To show $E_0 \notin \Omega(m)$, assume the opposite.

Since E_0 is a (saddle point), and by utilizing the Butler-McGhie lemma. There exists at least one point $n_0 \in \omega^s(E_0)$ and $\Omega(m)$, where $\omega^s(E_0)$ refers to the stable manifold of E_0.

Therefore, $\omega^s(E_0)$ indicated the $R_+^2(yz)$ space and $O(n_0)$ is the intact orbit through n_0 contained in $\Omega(m)$.

If n_0 is lying on the boundary axes of $R_+^2(yz)$, then the positive particular axis is contained in $\Omega(m)$, which implies to contradiction with boundedness.

If$n_0 \in Int.R_+^2(yz)$ and because non-presence of an equilibrium point in $Int.R_+^2(yz)$, the orbit through n_0 which contained in $\Omega(m)$ has to be un-bounded which implies to contradiction.

Thus, $E_0 \notin \Omega(m)$.
To show $E_1 \notin \Omega(m)$, assume the opposite as well.
Since E_1 is a (saddle point) if the condition (25) is met, and by utilizing the Butler-McGhie lemma, let $n_1 \in \omega^s(E_1) \cap \Omega(m)$. Moreover, $\omega^s(E_1)$ indicated the $R_+^2(xy)$ space (or $R_+^2(xz)$ space).
If n_1 is lying on the boundary axes of $R_+^2(xy)$, it implies to contradiction. If $n_1 \in Int. R_+^2(xy)$, and because the non-presence of an equilibrium point in $Int. R_+^2(xy)$, then $O(n_1) \subset \Omega(m)$ is unbounded which implies to contradicting with the bounded of $\Omega(m)$. Thus, $E_1 \notin \Omega(m)$.
To assure the persistence of system (1), Ω(m) has to be in the $Int. R_+^3$.

8. Bifurcation Analysis

A bifurcation occurs when the behavior of a dynamical system changes as a parameter is varied. The point at which this change occurs is referred to as the bifurcation parameter. Bifurcation analysis effectively measures qualitative changes in models, providing insight into the parameters where the model shifts from stable to unstable and vice versa.

Now, let's rephrase system (1) as follows: $\frac{d\boldsymbol{X}}{dt} = \boldsymbol{G}(\boldsymbol{X})$, where, $\boldsymbol{X} = (x, y, z)^T$ and $\boldsymbol{G} = (xg_1, g_2, g_3)^T$, with $g_1 = r\left(1 - \frac{x}{k}\right) - \frac{\beta_1 z}{1+\omega+\alpha x}$, $g_2 = \frac{e_1\beta_1 xz}{1+\omega+\alpha x} - \beta_2 yz - cy - d_1 y$ and $g_3 = cy + e_2\beta_2 yz - d_2 z$. Next, a straightforward computation on the Jacobian matrix of the system (1) with any non-zero vector $\boldsymbol{V} = (v_1, v_2, v_3)$ yields the second directional derivative as follows:

$$D^2\boldsymbol{G}(\boldsymbol{X})(\boldsymbol{V}, \boldsymbol{V}) = (M_{i1})_{3\times 1}. \tag{26}$$

Where, $M_{11} = (\frac{-2r}{k} + \frac{2(1+\omega)\alpha\beta_1 z}{(1+\omega+\alpha x)^3})v_1^2 - \frac{2(1+\omega)\beta_1}{(1+\omega+\alpha x)^2} v_1 v_3$, $M_{21} = \frac{-2(1+\omega)e_1\alpha\beta_1 z}{(1+\omega+\alpha x)^3} v_1^2 + \frac{2(1+\omega)e_1\beta_1}{(1+\omega+\alpha x)^2} v_1 v_3 - 2\beta_2 v_2 v_3$, $M_{31} = 2e_2\beta_2 v_2 v_3$.

Sequentially, the third directional derivative is as follows:

$$D^3\boldsymbol{G}(\boldsymbol{X})(\boldsymbol{V}, \boldsymbol{V}, \boldsymbol{V}) = (N_{i1})_{3\times 1}. \tag{27}$$

Where, $N_{11} = \frac{-6(1+\omega)\alpha^2\beta_1 z}{(1+\omega+\alpha x)^4} v_1^3 + \frac{6(1+\omega)\alpha\beta_1}{(1+\omega+\alpha x)^3} v_1^2 v_3$, $N_{21} = \frac{6(1+\omega)e_1\alpha^2\beta_1 z}{(1+\omega+\alpha x)^4} v_1^3 - \frac{6(1+\omega)e_1\alpha\beta_1}{(1+\omega+\alpha x)^3} v_1^2 v_3$, $N_{31} = 0$.

So, to examine the occurrence of bifurcations at equilibrium points, the conditions of Sotomayor's Theorem [38] must be verified, and according to it, at a bifurcation point, one eigenvalue of the Jacobian matrix must be zero.

Theorem 6. System (1) around the A-EP undergoes a transcritical bifurcation when the parameter

d_2 possesses the value $d_2^* = \frac{ce_1\beta_1 k}{(c+d_1)(1+\omega+\alpha k)}$ and the following condition is met.

$$\delta\left(\frac{(1+\omega)e_1\beta_1}{(1+\omega+\alpha k)^2}\gamma_1 - \beta_2\gamma_2\right) + e_2\beta_2\gamma_2 \neq 0. \tag{28}$$

Otherwise, pitchfork bifurcation occurs, where γ_1 and γ_2 are specified in the proof.

Proof. From Eq. (8), system (1) at A-EP and d_2^* can be written as

$$J(E_1, d_2^*) = \begin{pmatrix} -r & 0 & -\frac{k\beta_1}{1+\omega+\alpha k} \\ 0 & -(c+d_1) & \frac{ke_1\beta_1}{1+\omega+\alpha k} \\ 0 & c & -\frac{ce_1\beta_1 k}{(c+d_1)(1+\omega+\alpha k)} \end{pmatrix}. \tag{29}$$

So, the A-EP is a non-hyperbolic point and $J(E_1, d_2^*)$ has a zero eigenvalue in the z −direction referred to as λ_z.

Here, let $\boldsymbol{V} = (\gamma_1 v_3, \gamma_2 v_3, v_3)$ be the eigenvector of $J(E_1, d_2^*)$, where v_3 represents any non-zero real number, $\gamma_1 = -\frac{k\beta_1}{r(1+\omega+\alpha k)} < 0$, $\gamma_2 = \frac{ke_1\beta_1}{(c+d_1)(1+\omega+\alpha k)} > 0$ and let $\boldsymbol{W} = (0, \delta w_3, w_3)^T$ be the eigenvector of $J(E_1, d_2^*)^T$, where w_3 represents any non-zero real number, $\delta = \frac{c}{c+d_1} > 0$.

Now, $\frac{\partial \boldsymbol{G}}{\partial d_2} = (0,0,-z)$.

$\boldsymbol{W}^T.\boldsymbol{G}_{d_2}(E_1, d_2^*) = 0$. Therefore, system (1) has no saddle-node bifurcation at d_2^*.

Moreover, $\boldsymbol{W}^T[D\boldsymbol{G}_{d_2}(E_1, d_2^*)\boldsymbol{V}] = -w_3 v_3 \neq 0$.

Hence, by utilizing Eq. (26) with E_1, d_2^* and $\boldsymbol{V}$, it's obtained

$$\boldsymbol{W}^T[D^2\boldsymbol{G}(E_1, d_2^*)(\boldsymbol{V},\boldsymbol{V})] = 2w_3 v_3^2\left(\delta\left(\frac{(1+\omega)e_1\beta_1}{(1+\omega+\alpha k)^2}\gamma_1 - \beta_2\gamma_2\right) + e_2\beta_2\gamma_2\right).$$

Then, by Sotomayor's theorem, system (1) undergoes a transcritical bifurcation around d_2^* when the condition (28) holds, but if the condition (28) fails, utilizing Eq. (27) with E_1, d_2^* and $\boldsymbol{V}$, it's obtained

$$\boldsymbol{W}^{\boldsymbol{T}}[D^3\boldsymbol{G}(E_1, d_2^*)(\boldsymbol{V},\boldsymbol{V},\boldsymbol{V})] = -6w_3 v_3^3\left(\frac{(1+\omega)e_1\alpha\beta_1}{(1+\omega+\alpha k)^3}\gamma_1^2\delta\right) \neq 0.$$

Thus, the proof is completed, and the pitchfork bifurcation occurs.

Theorem 7. Provided that conditions (14) and (16) are satisfied, system (1) undergoes a saddle-node bifurcation at the COE-EP with the bifurcation parameter $r^* = \frac{k}{x^*}\left(\frac{\alpha\beta_1 x^* z^*}{(1+\omega+\alpha x^*)^2} - \Phi\right)$, where $\Phi = \frac{\epsilon_{13}\epsilon_{21}\epsilon_{32}}{\epsilon_{23}\epsilon_{32} - \epsilon_{22}\epsilon_{33}} > 0$ and the following condition is met.

$\sigma_1\rho_1\left[\left(\frac{-r}{k}+\frac{(1+\omega)\alpha\beta_1 z^*}{(1+\omega+\alpha x^*)^3}\right)\sigma_1-\frac{(1+\omega)\beta_1}{(1+\omega+\alpha x^*)^2}\right]+\rho_2\left[\sigma_1\left(\frac{-(1+\omega)e_1\alpha\beta_1 z^*}{(1+\omega+\alpha x^*)^3}\sigma_1+\frac{(1+\omega)e_1\beta_1}{(1+\omega+\alpha x^*)^2}\right)-\beta_2\sigma_2\right]+$

$e_2\beta_2\,\sigma_2\neq 0.$ (30)

Proof. From Eq. (11), system (1) at COE-EP, and r^* can be written as

$$J(E_2,r^*)=\begin{pmatrix}\Phi & 0 & \epsilon_{13}\\ \epsilon_{21} & \epsilon_{22} & \epsilon_{23}\\ 0 & \epsilon_{32} & \epsilon_{33}\end{pmatrix}. \tag{31}$$

Now, from the characteristic equation (12), system (1) has a zero eigenvalue at r^* if $A_3=0$, and then the COE-EP is a non-hyperbolic point and $J(E_2,r^*)$ has zero eigenvalue in the $x-$direction referred by λ_x.

Now, let $\boldsymbol{V}=(\sigma_1 v_3,\sigma_2 v_3,v_3)^T$ be the eigenvector of $J(E_2,r^*)$, where v_3 represents any non-zero real number and $\sigma_1=-\frac{\epsilon_{13}}{\Phi}$, $\sigma_2=\frac{\epsilon_{13}\epsilon_{21}-\Phi\epsilon_{23}}{\Phi\epsilon_{22}}$. Let $\boldsymbol{W}=(\rho_1 w_3,\rho_2 w_3,w_3)^T$ be the eigenvector of $J(E_2,r^*)^T$, where w_3 represents any non-zero real number and $\rho_1=\frac{\epsilon_{21}\epsilon_{32}}{\Phi\epsilon_{22}}$, $\rho_2=\frac{\epsilon_{32}}{\epsilon_{22}}$. So, $\boldsymbol{W}^T\boldsymbol{G}_r(E_2,r^*)=x^*(1-\frac{x^*}{k})\rho_1 w_3\neq 0$. Therefore, system (1) has a first condition of saddle-node bifurcation at r^*.

Hence, by utilising Eq. (26) with E_2, r^* *and* $\boldsymbol{V}$, it's obtained

$$\boldsymbol{W}^T[D^2\boldsymbol{G}(E_2,r^*)(\boldsymbol{V},\boldsymbol{V})]=2w_3v_3^2\Big\{\sigma_1\rho_1\left[\left(\frac{-r}{k}+\frac{(1+\omega)\alpha\beta_1 z^*}{(1+\omega+\alpha x^*)^3}\right)\sigma_1-\frac{(1+\omega)\beta_1}{(1+\omega+\alpha x^*)^2}\right]+$$
$$\rho_2\left[\sigma_1\left(\frac{-(1+\omega)e_1\alpha\beta_1 z^*}{(1+\omega+\alpha x^*)^3}\sigma_1+\frac{(1+\omega)e_1\beta_1}{(1+\omega+\alpha x^*)^2}\right)-\beta_2\sigma_2\right]+e_2\beta_2\,\sigma_2\Big\}.$$

Then, by Sotomayor's theorem, system (1) undergoes a saddle-node bifurcation around the COE-EP at r^* when the condition (30) is met.

9. NUMERICAL ANALYSIS

The numerical analysis displays a frame for simulating complex interactions between the species and their environment; it is major to our knowledge of ecological models. Utilizing these analyses, investigators can predict results and the behavior of dynamical systems.

Now, System (1) is numerically resolved utilizing a guess set of biologically feasible parameter values, listed below in Table 2, with six different sets of initial values and the assistance of the MATLAB program; the results are then offered as time series and phase portraits.

Table 2. Default parameter values.

Parameters	r	k	β_1	ω	α	e_1	β_2	c	d_1	e_2	d_2
Values	2	20	0.6	2	0.25	0.6	0.1	0.1	0.1	0.4	0.3

Note that the trajectory of system (1) beginning from the different initial points utilizing the parameters in Table 2 approaches asymptotically, $E_2 = (11.9, 5.7, 8.1)$ as illustrated in Figure 1.

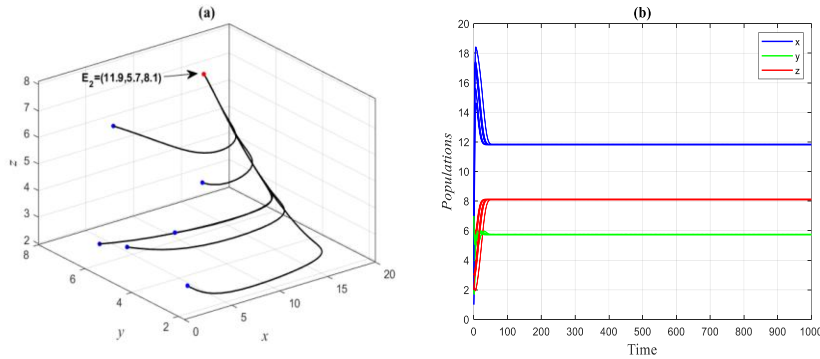

Figure 1. The trajectory using the parameter values in Table 2. (a) The phase portrait from different initial points. (b) Illustrates the time series of (a).

The impact of altering the values of the parameter r on the system dynamics (1) is explained in Figure 2. As shown in Figure 2., if the parameter r is increasing (decreasing), then the predators (mature and immature) will increase (decrease) too. Also, the trajectory is approaching E_2 in the $int.R^3_+$.

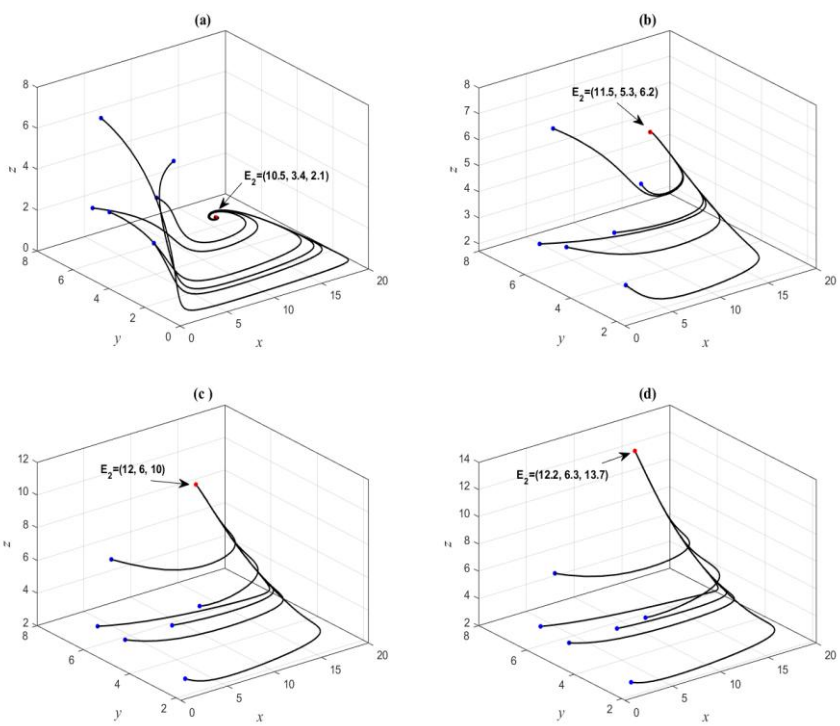

Figure 2. The trajectory using the parameter values in Table 2 and different values of r. (a) For $r = 0.5$. (b) For $r = 1.5$. (c) For $r = 2.5$. (d) For $r = 3.5$

Now, the effect of altering the values of the parameter k on the system dynamics (1) is illustrated in Figure 3. It is clear that the trajectory is approaching E_1, E_2, and periodic oscillation in the $int.R^3_+$. in the ranges $1 \leq k < 9$, $9 \leq k < 33$ and $33 \leq k$, respectively.

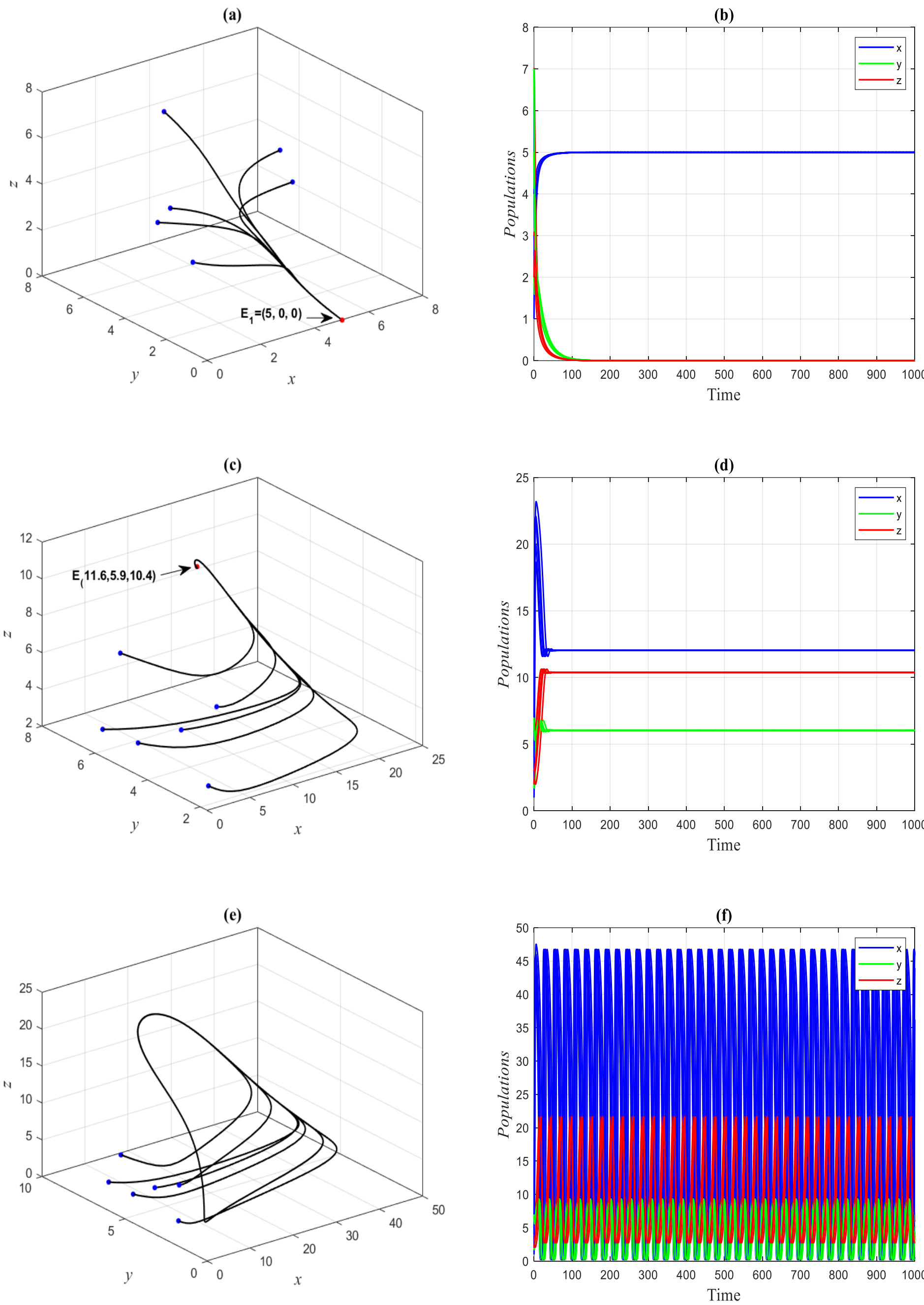

Figure 3. The trajectory using the parameter values in Table 2 and different values of k. (a) For $k = 5$. (b) Illustrates the time series of (a). (c) For $k = 25$. (d) Illustrates the time series of (c). (e) For $k = 50$. (f) Illustrates the time series of (e).

In Figure 4, the effect of altering the values of the parameter β_1 on the system dynamics (1) is clarified. It is observed that the trajectory is approaching E_1, E_2, and periodic oscillation in the $int.R^3_+$. in the ranges $0.01 \leq \beta_1 < 0.4$, $0.4 \leq \beta_1 < 0.84$ and $0.84 \leq \beta_1$, respectively.

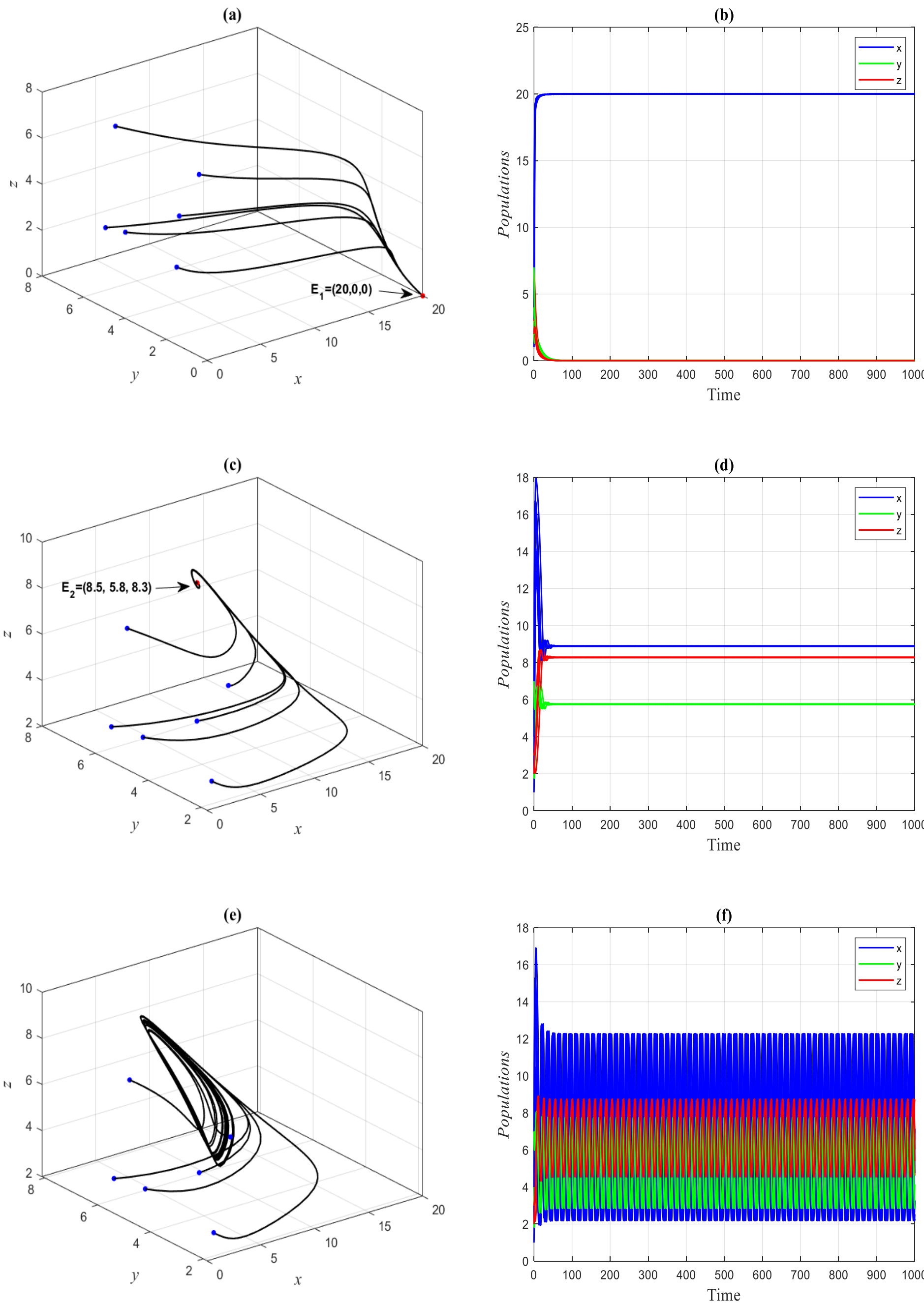

Figure 4. The trajectory using the parameter values in Table 2 and different values of β_1. (a) For $\beta_1 = 0.2$. (b) Illustrates the time series of (a). (c) For $\beta_1 = 0.7$. (d) Illustrates the time series of (c). (e) For $\beta_1 = 0.9$. (f) Illustrates the time series of (e).

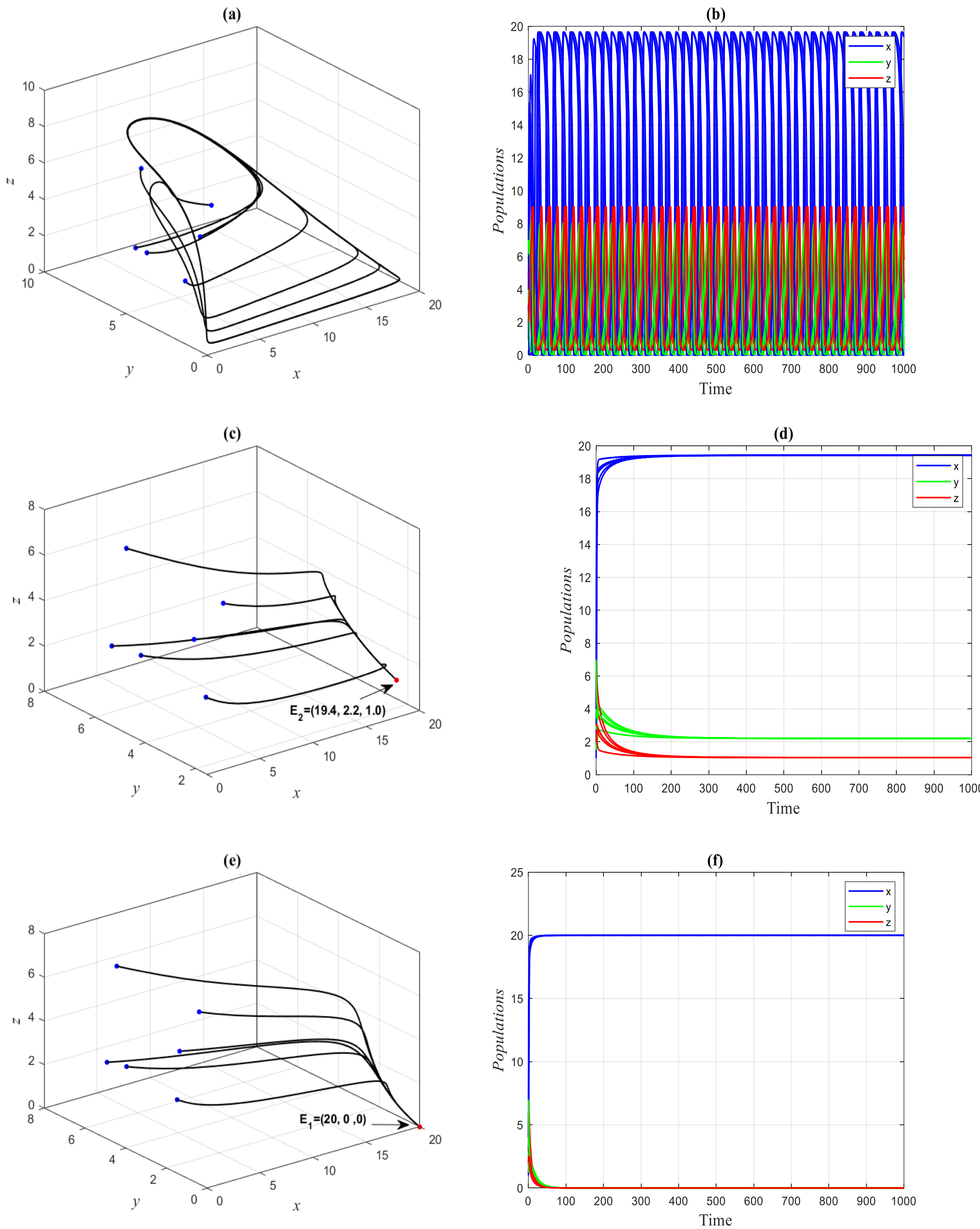

Figure 5. The trajectory using the parameter values in Table 2 and different values of ω. (a) For $\omega = 0$. (b) Illustrates the time series of (a). (c) For $\omega = 5$. (d) Illustrates the time series of (c). (e) For $\omega = 15$. (f) Illustrates the time series of (e).

Clearly, the effect of altering the values of the parameter ω on the system dynamics (1) is illustrated in Figure 5 It is observe that the trajectory is approaching periodic oscillation in the $int.R^3_+$., E_2 and E_1 in the ranges $0 \le \omega < 1$, $1 \le \omega < 7$ and $7 \le \omega$, respectively.

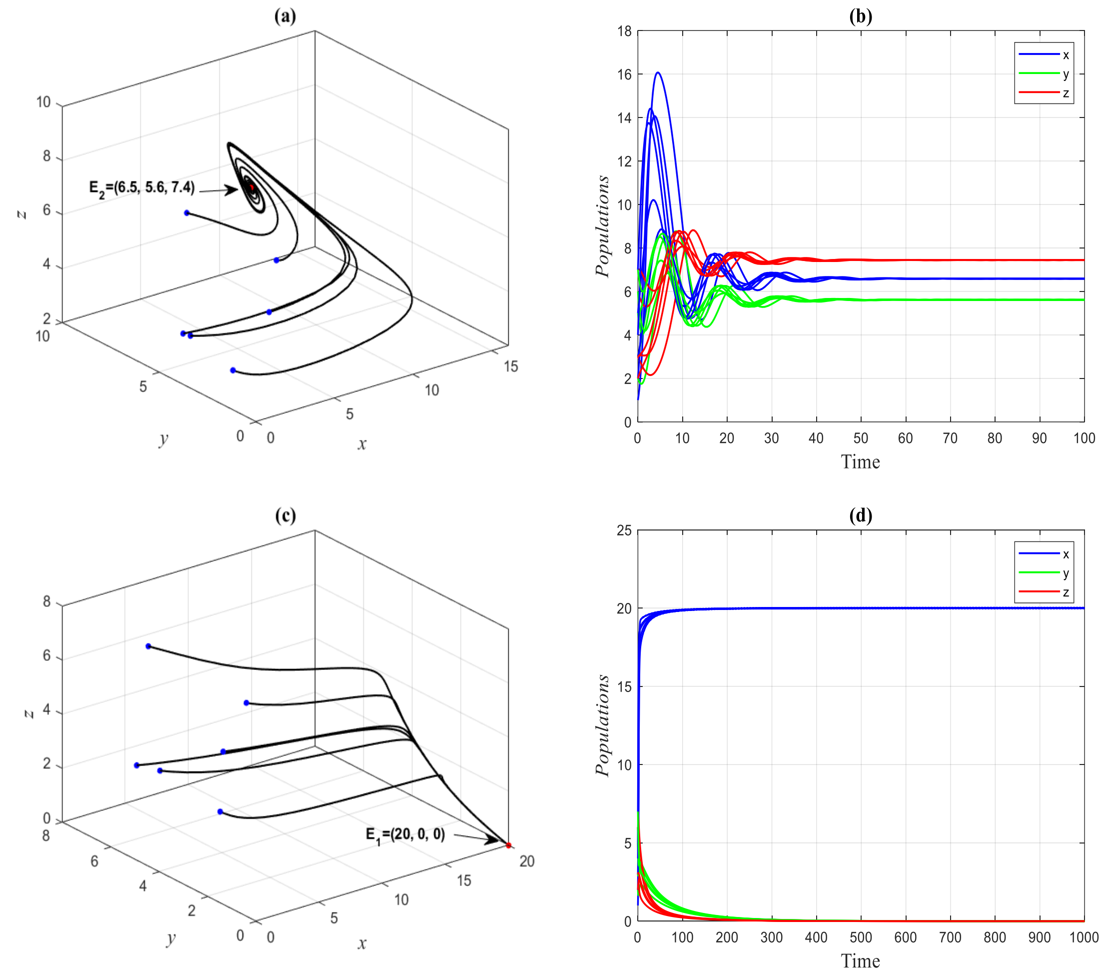

Figure 6. The trajectory using the parameter values in Table 2 and different values of α. (a) For $\alpha = 0..05$ (b) Illustrates the time series of (a). (c) For $\alpha = 0.5$. (d) Illustrates the time series of (c).

In Figure 6, the effect of altering the values of the parameter α on the system dynamics (1) is clarified. The trajectory is approaching E_2 and E_1 in the ranges $0.001 \le \alpha < 0.2$ and $0.2 \le \alpha$, respectively.

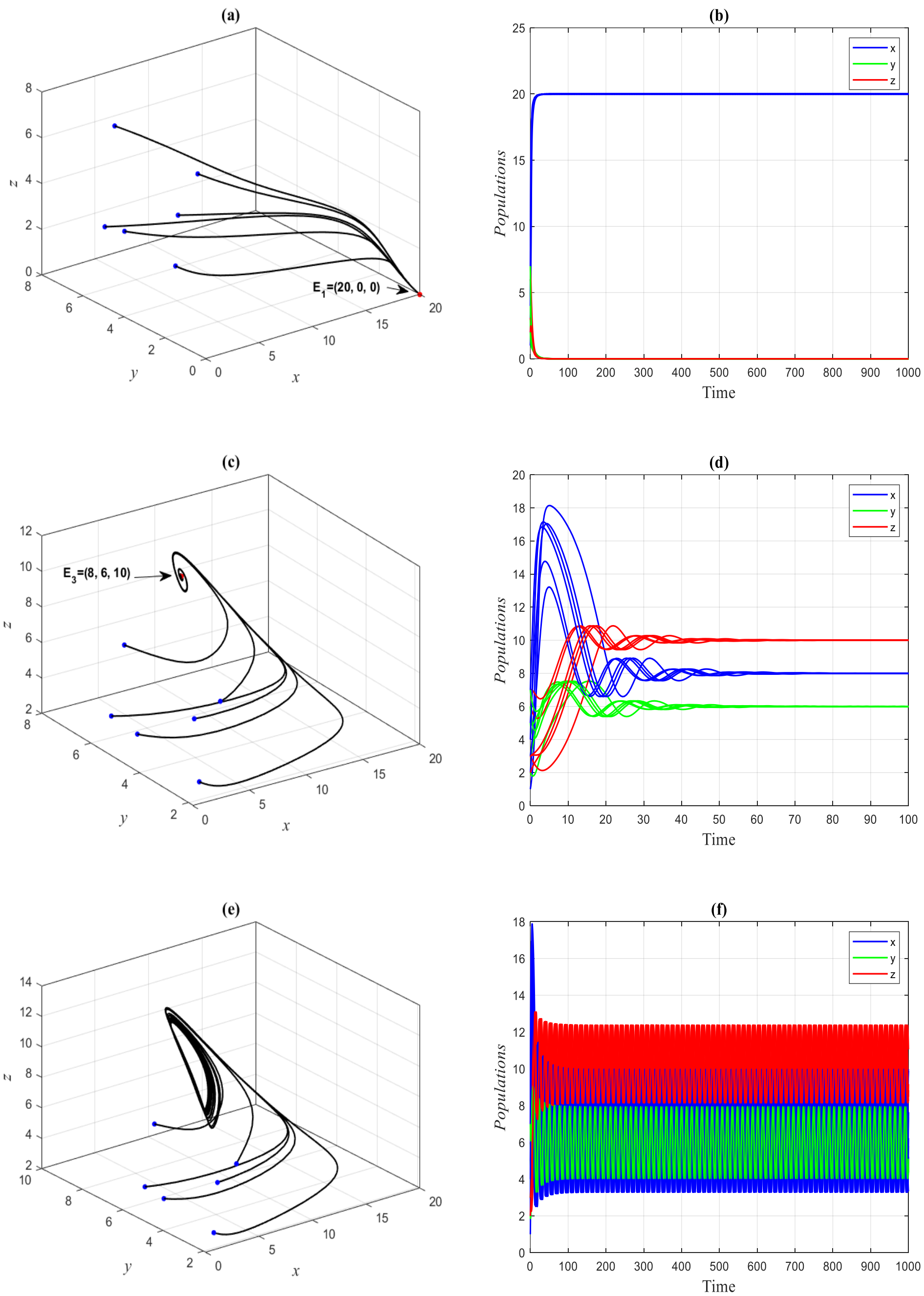

Figure 7. The trajectory using the parameter values in Table 2 and different values of e_1. (a) For $e_1 = 0.1$. (b) Illustrates the time series of (a). (c) For $e_1 = 0.75$. (d) Illustrates the time series of (c). (e) For $e_1 = 0.9$. (f) Illustrates the time series of (e).

In Figure 7, altering the values of the parameter e_1 in the ranges $0.01 \leq e_1 < 0.4$, $0.4 \leq e_1 < 0.86$ and $0.86 \leq e_1$ make the system (1) approach E_1, E_2 and periodic oscillation in the $int.R^3_+$. for chose values.

The effect of altering the values of the parameter β_2 of system (1) is a quantitative effect and the trajectory undergoes to E_2.

Clearly, the effect of altering the values of the parameter c on the system dynamics (1) is illustrated in Figure 8 It is observe that the trajectory is approaching E_1 in the range $0.01 \leq c < 0.03$. For $0.03 \leq c < 0.04$, the trajectory is approaching two different attractors E_1 and E_2, that means appearing of bi-stable state. For $0.04 \leq c$, then the trajectory is approaching E_2.

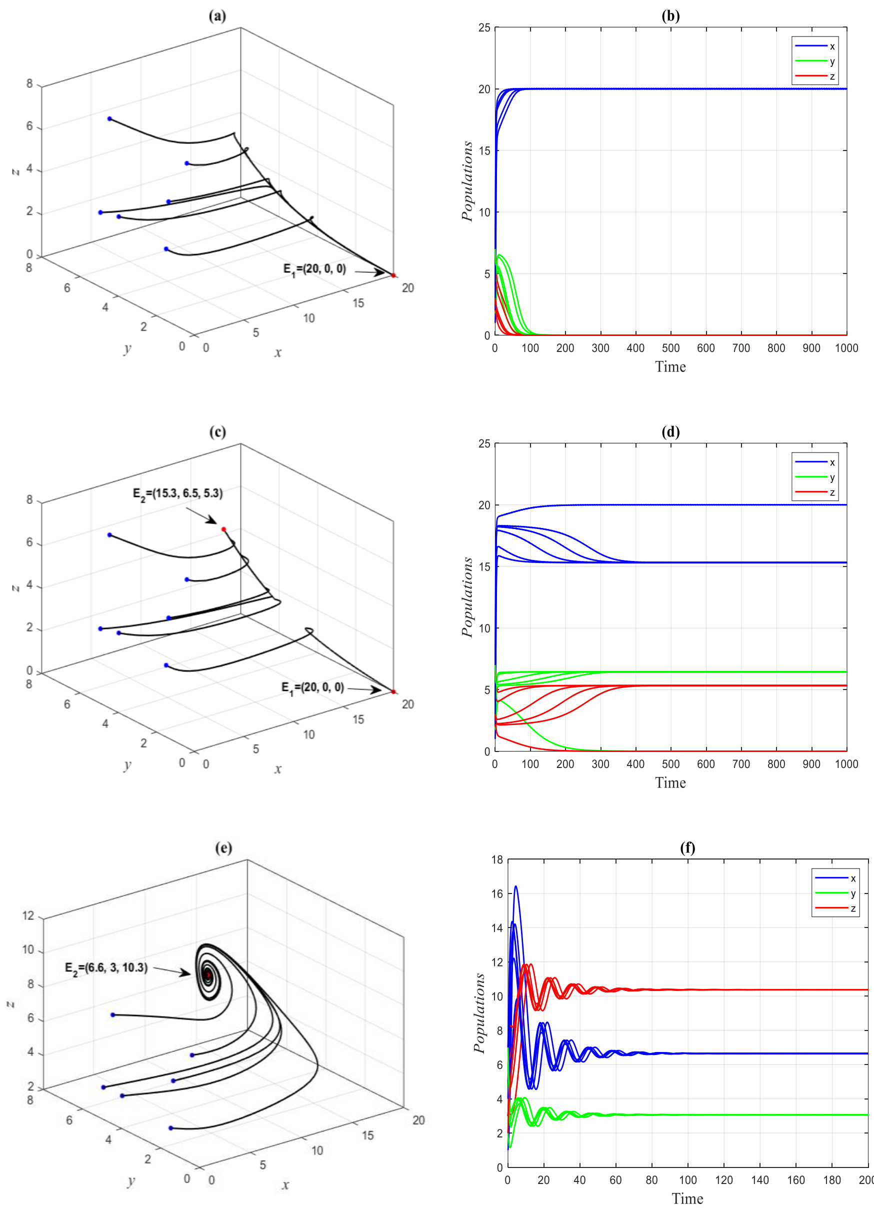

Figure 8. The trajectory using the parameter values in Table 2 and different values of c. (a) For $c = 0.02$. (b) Illustrates the time series of (a). (c) For $c = 0.035$. (d) Illustrates the time series of (c). (e) For $c = 0.6$. (f) Illustrates the time series of (e).

Now, the effect of altering the values of the parameter d_1 on the system dynamics (1) is illustrated in Figure 9. It is clear that the trajectory is approaching E_2 and E_1 in the ranges $0.01 \leq d_1 < 0.2$, $0.2 \leq d_1$, respectively.

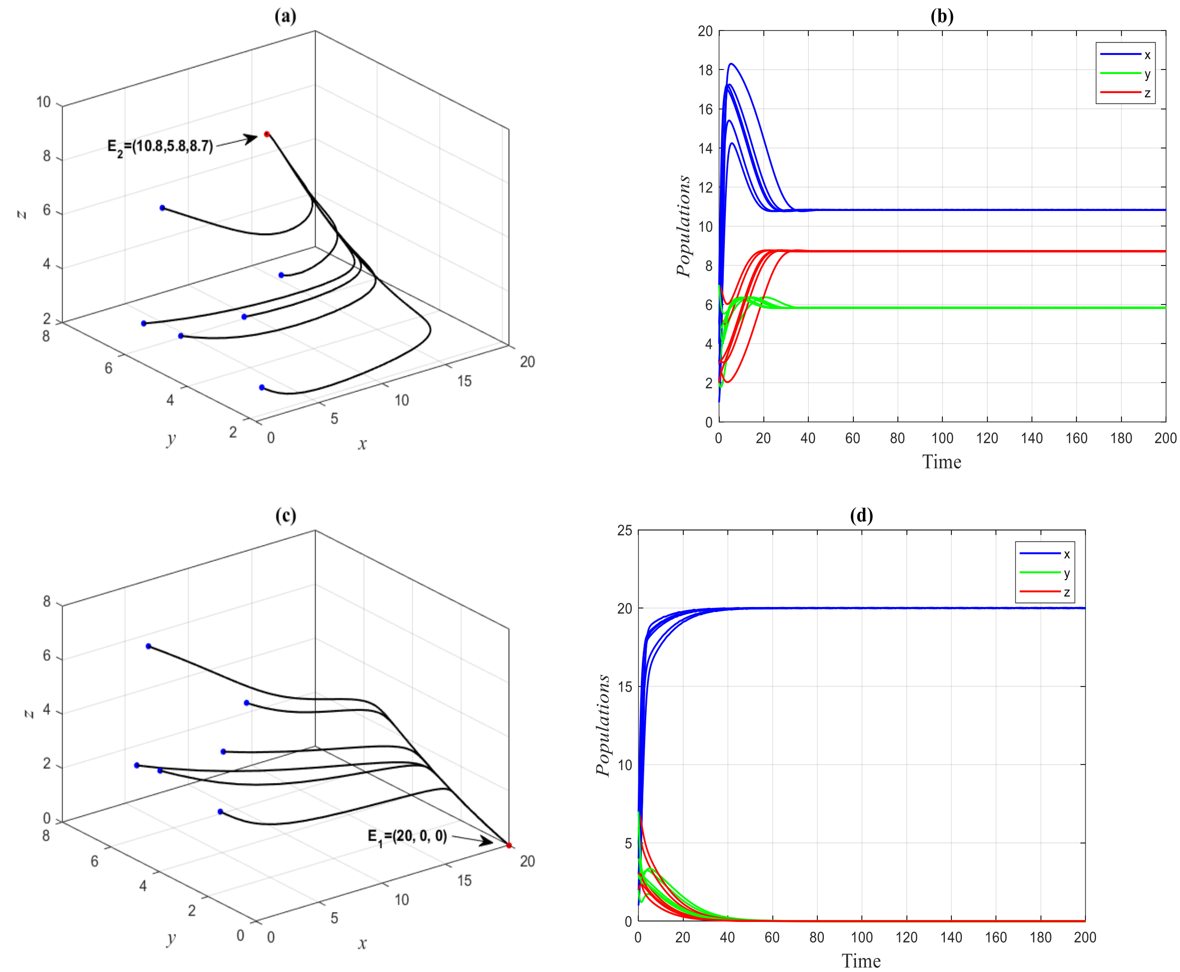

Figure 9. The trajectory using the parameter values in Table 2 and different values of d_1. (a) For $d_1 = 0.05$. (b) Illustrates the time series of (a). (c) For $d_1 = 0.5$. (d) Illustrates the time series of (c).

In Figure 10, the effect of altering the values of the parameter e_2 on the system dynamics (1) is clarified. It is observed that the trajectory is approaching E_2 and periodic oscillation in the $int.R_+^3$. in the ranges $0.01 \leq e_2 < 0.61$ and $0.61 \leq e_2$, respectively.

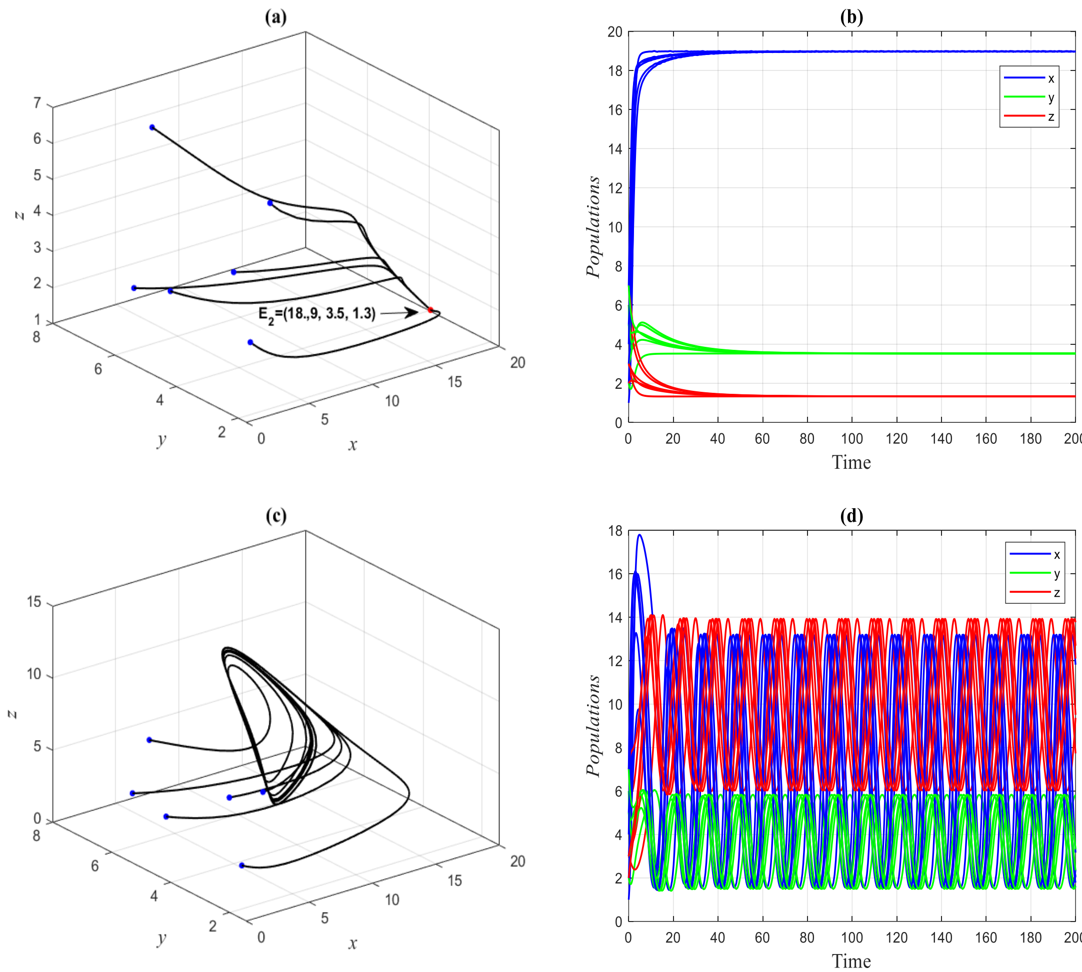

Figure 10. The trajectory using the parameter values in Table 2 and different values of e_2. (a) For $e_2 = 0.1$. (b) Illustrates the time series of (a). (c) For $e_2 = 0.7$. (d) Illustrates the time series of (c).

Finally, the effect of altering the values of the parameter d_2 on the system dynamics (1) is illustrated in Figure 11 It is observed that the trajectory is approaching periodic oscillation in the $int.R_+^3$, E_2 and E_1 in the ranges $0.01 \leq d_2 < 0.2$, $0.2 \leq d_2 < 0.5$, and $0.5 \leq d_2$ respectively.

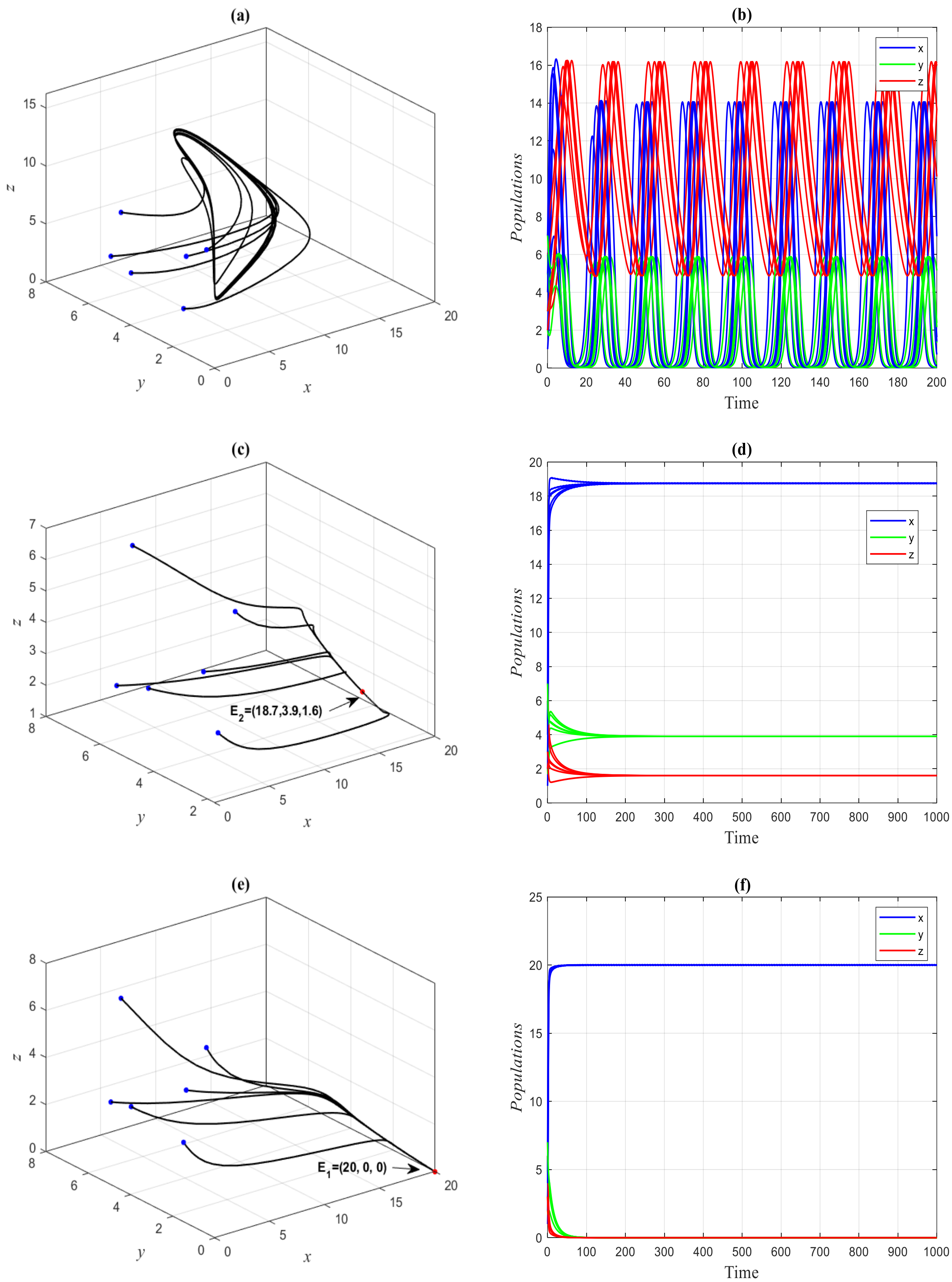

Figure 11. The trajectory using the parameter values in Table 2 and different values of d_2. (a) For $d_2 = 0.1$. (b) Illustrates the time series of (a). (c) For $d_2 = 0.4$. (d) Illustrates the time series of (c). (e) For $d_2 = 0.7$. (f) Illustrates the time series of (e).

10. CONCLUSIONS

This article has examined a stage structured predator–prey system that contains cannibalism in the predators. The effect of wind on the dynamics of the system is studied. The solution's properties of the system are explained, the existence and stability of equilibrium points are studied, and the persistence is investigated. Also, the local bifurcation around the possible equilibrium points is studied. The suggested system is solved numerically by using different initial points and a set of parameters as shown in Table 2.

It is noted that the system contains different types of dynamics, and the results are summarized as follows:

Depending on the initial values and using the parameter values in Table 2, it was being noted that the trajectory of system (1) was approaching E_2 in the $int. R_+^3$. Due to the increasing (decreasing) of intrinsic growth rate values, the number of predators (mature and immature) increased (decreased). On the other hand, the carrying capacity k, the attack rate β_1 and the conversion rate e_1 have the same effect on the dynamic of system (1). It is clear that, the trajectory is approaching E_1, E_2 and periodic oscillation in the $int. R_+^3$. While the effect of wind flow ω and the mortality rate of mature predator d_2 have the same action on the dynamic of system (1). It is noted that, the trajectory is approaching periodic oscillation in the $int. R_+^3$, E_2 and E_1, which indicate the opposite effect to k, β_1 and e_1. Also, the effect of wind flow ω and the mortality rate of mature predator d_2 have the same action on the dynamic of system (1). Moreover, the impact of the hindrance rate α and the mortality rate of immature predator d_1 have the same effect on the dynamic of system (1). The trajectory is approaching E_2 and E_1. Increasing (decreasing) the values of the attack rate of mature predator β_2 below (above) the particular value leads to the trajectory approaching E_2, that means quantitative effects of the system. Finally, the trajectory is sensitive to change in the rate of growth from an immature predator into a mature predator c. The trajectory is approaching E_1 and then converting to a bi-stable state (E_1 & E_2) and then to E_2 in the $int. R_+^3$. As a result, System (1) is sensitive to alterations in the biological parameter's values.

In this article, the future direction will be shown as follows: For the proposed model, which contains the stage structure, wind flow and cannibalism, it is possible to develop it by using different types of functional responses and biological factors.

CONFLICT OF INTERESTS

The authors declare that there is no conflict of interests.

REFERENCES

[1] A.J. Lotka, Elements of Physical Biology, Williams and Wilkins, Baltimore, 1925.

[2] V. Volterra, Fluctuations in the Abundance of a Species Considered Mathematically, Nature 118 (1926), 558-560. https://doi.org/10.1038/118558a0.

[3] N.H. Fakhry, R.K. Naji, Fear and Hunting Cooperation's Impact on the Eco-Epidemiological Model's Dynamics, Int. J. Anal. Appl. 22 (2024), 15. https://doi.org/10.28924/2291-8639-22-2024-15.

[4] D.K. Bahlool, The Dynamics of a Stage-Structure Prey-Predator Model with Hunting Cooperation and Anti-Predator Behavior, Commun. Math. Biol. Neurosci. 2023 (2023), 59. https://doi.org/10.28919/cmbn/8003.

[5] A.R.M. Jamil, R.K. Naji, Modeling and Analyzing the Influence of Fear on the Harvested Modified Leslie-Gower Model, Baghdad Sci. J. 20 (2023), 1701-1712. https://doi.org/10.21123/bsj.2023.7432.

[6] H.A. Ibrahim, R.K. Naji, The Impact of Fear on a Harvested Prey–Predator System with Disease in a Prey, Mathematics 11 (2023), 2909. https://doi.org/10.3390/math11132909.

[7] B.E. Kashem, H.F. Al-Husseiny, The Dynamic of Two Prey–One Predator Food Web Model with Fear and Harvesting, Partial Differ. Equ. Appl. Math. 11 (2024), 100875. https://doi.org/10.1016/j.padiff.2024.100875.

[8] W.M. Alwan, H.A. Satar, The Effects of Media Coverage on the Dynamics of Disease in Prey-Predator Model, Iraqi J. Sci. 62 (2021), 981-996. https://doi.org/10.24996/ijs.2021.62.3.28.

[9] H.A. Ibrahim, On the Dynamical Behavior of an Eco-Epidemiological Model, Int. J. Nonlinear Anal. Appl. 12 (2021), 1749-1767. https://doi.org/10.22075/ijnaa.2021.5314.

[10] D.K. Bahlool, H.A. Satar, H.A. Ibrahim, Order and Chaos in a Prey-Predator Model Incorporating Refuge, Disease, and Harvesting, J. Appl. Math. 2020 (2020), 5373817. https://doi.org/10.1155/2020/5373817.

[11] F.H. Maghool, R.K. Naji, The Effect of Fear on the Dynamics of Two Competing Prey-One Predator System Involving Intra-Specific Competition, Commun. Math. Biol. Neurosci. 2022 (2022), 42. https://doi.org/10.28919/cmbn/7376.

[12] M.S. Shabbir, Q. Din, M. De la Sen, J.F. Gómez-Aguilar, Exploring Dynamics of Plant–Herbivore Interactions: Bifurcation Analysis and Chaos Control with Holling Type-II Functional Response, J. Math. Biol. 88 (2024), 8. https://doi.org/10.1007/s00285-023-02020-5.

[13] S.L. Cheru, K.G. Kebedow, T.T. Ega, Prey-Predator Model of Holling Type II Functional Response with Disease on Both Species, Differ. Equ. Dyn. Syst. 34 (2026), 131-154. https://doi.org/10.1007/s12591-024-00677-y.

[14] B.B. Kamal, A. Mustafa, Dynamical Analysis of a Three Species Food-Web Model with Extended Holling Type II Functional Response, Eur. J. Pure Appl. Math. 18 (2025), 5397. https://doi.org/10.29020/nybg.ejpam.v18i1.5397.

[15] H. Deng, F. Chen, Z. Zhu, Z. Li, Dynamic Behaviors of Lotka–Volterra Predator–Prey Model Incorporating

Predator Cannibalism, Adv. Differ. Equ. 2019 (2019), 359. https://doi.org/10.1186/s13662-019-2289-8.

[16] N. Kumari, V. Kumar, Controlling Chaos and Pattern Formation Study in a Tritrophic Food Chain Model with Cannibalistic Intermediate Predator, Eur. Phys. J. Plus 137 (2022), 345. https://doi.org/10.1140/epjp/s13360-022-02539-4.

[17] M. Rayungsari, A. Suryanto, W.M. Kusumawinahyu, I. Darti, Dynamical Analysis of a Predator-Prey Model Incorporating Predator Cannibalism and Refuge, Axioms 11 (2022), 116. https://doi.org/10.3390/axioms11030116.

[18] F. Cunha-Saraiva, S. Balshine, R.H. Wagner, F.C. Schaedelin, From Cannibal to Caregiver: Tracking the Transition in a Cichlid Fish, Anim. Behav. 139 (2018), 9-17. https://doi.org/10.1016/j.anbehav.2018.03.003.

[19] T.M. Canales, G.W. Delius, R. Law, Regulation of Fish Stocks without Stock–Recruitment Relationships: The Case of Small Pelagic Fish, Fish Fish. 21 (2020), 857-871. https://doi.org/10.1111/faf.12465.

[20] A.M. Koltz, J.P. Wright, Impacts of Female Body Size on Cannibalism and Juvenile Abundance in a Dominant Arctic Spider, J. Anim. Ecol. 89 (2020), 1788-1798. https://doi.org/10.1111/1365-2656.13230.

[21] S. Zhang, L. Yu, M. Tan, N.Y.L. Tan, X.X.B. Wong, et al., Male Mating Strategies to Counter Sexual Conflict in Spiders, Commun. Biol. 5 (2022), 534. https://doi.org/10.1038/s42003-022-03512-8.

[22] C. Trapanese, M. Bey, G. Tonachella, H. Meunier, S. Masi, Prolonged Care and Cannibalism of Infant Corpse by Relatives in Semi-Free-Ranging Capuchin Monkeys, Primates 61 (2020), 41-47. https://doi.org/10.1007/s10329-019-00747-8.

[23] P. Oliva-Vidal, J. Tobajas, A. Margalida, Cannibalistic Necrophagy in Red Foxes: Do the Nutritional Benefits Offset the Potential Costs of Disease Transmission?, Mamm. Biol. 101 (2021), 1115-1120. https://doi.org/10.1007/s42991-021-00184-5.

[24] H.A. Ibrahim, R.K. Naji, The Complex Dynamic in Three Species Food Web Model Involving Stage Structure and Cannibalism, AIP Conf. Proc. 2292 (2020), 020006. https://doi.org/10.1063/5.0030510.

[25] A.S. Abdulghafour, R.K. Naji, The Significance of Cannibalism, Panic, and Sanctuary in the Interactions Between Prey and Predator with a Stage Structure, Iraq. J. Comput. Sci. Math. 5 (2024), 16. https://doi.org/10.52866/2788-7421.1206.

[26] G.J. Abdulsada, H.A. Ibrahim, The Role of Fear and Predator Dependent Refuge on a Stage Structure Prey-Predator System, Baghdad Sci. J. 22 (2025), 1660-1679. https://doi.org/10.21123/2411-7986.4970.

[27] N. Mondal, D. Barman, S. Alam, Impact of Adult Predator Incited Fear in a Stage-Structured Prey–Predator Model, Environ. Dev. Sustain. 23 (2021), 9280-9307. https://doi.org/10.1007/s10668-020-01024-1.

[28] E.M. Takyi, K. Antwi-Fordjour, Counter-Attack in a Stage-Structured Model with Adult Predator-Induced Fear and Competition, Int. J. Dyn. Control 11 (2023), 2720-2732. https://doi.org/10.1007/s40435-023-01193-7.

[29] P.S. Harine, A. Kumar, S.K. Sasmal, Complex Dynamics of a Stage Structured Prey-Predator Model with Parental Care in Prey, Nonlinear Dyn. 112 (2024), 15623-15649. https://doi.org/10.1007/s11071-024-09821-3.

[30] S. Bentout, S. Djilali, A. Atangana, Bifurcation Analysis of an Age-Structured Prey–Predator Model with Infection Developed in Prey, Math. Methods Appl. Sci. 45 (2022), 1189-1208. https://doi.org/10.1002/mma.7846.

[31] K. Manimaran, F. Mustapha, F. Mohd Siam, Intraguild Predation (IGP) Model with Stage Structure and Cannibalism in Predator Population, AIP Conf. Proc. 3023 (2024), 030030. https://doi.org/10.1063/5.0171695.

[32] P. Panja, Impacts of Wind and Anti-Predator Behaviour on Predator-Prey Dynamics: A Modelling Study, Int. J. Comput. Sci. Math. 15 (2022), 396-407. https://doi.org/10.1504/ijcsm.2022.125906.

[33] R.A. Ali, H.A. Ibrahim, Role of Wind and Fear on the Dynamic of a Prey and Two Competing Predators, J. Appl. Math. 2025 (2025), 3756733. https://doi.org/10.1155/jama/3756733.

[34] K.I. Hadib, H.A. Ibrahim, The Dynamic of a Three Species Food Chain Model under the Influence of Fear and Wind, Baghdad Sci. J. 22 (2025), 3805-3824. https://doi.org/10.21123/2411-7986.5123.

[35] R.A. Ali, H.A. Ibrahim, Effect of Wind and Disease on the Dynamical Behavior of a Prey-Predator System, Commun. Math. Biol. Neurosci. 2025 (2025), 84. https://doi.org/10.28919/cmbn/9305.

[36] D. Barman, J. Roy, S. Alam, Impact of Wind in the Dynamics of Prey–Predator Interactions, Math. Comput. Simul. 191 (2022), 49-81. https://doi.org/10.1016/j.matcom.2021.07.022.

[37] J.D. Murray, Mathematical Biology, Springer Berlin Heidelberg, Berlin, 1989. https://doi.org/10.1007/978-3-662-08539-4.

[38] L. Perko, Differential Equations and Dynamical Systems, 3rd ed., Texts in Applied Mathematics, vol. 7, Springer, New York, 2001. https://doi.org/10.1007/978-1-4613-0003-8.